Measurement of the Mass Difference Between Neutral Charm-Meson Eigenstates

R. Aaij *et al.*[*]
(LHCb Collaboration)

(Received 8 March 2019; published 14 June 2019)

We report a measurement of the mass difference between neutral charm-meson eigenstates using a novel approach that enhances sensitivity to this parameter. We use 2.3×10^6 $D^0 \to K^0_S\pi^+\pi^-$ decays reconstructed in proton-proton collisions collected by the LHCb experiment in 2011 and 2012. Allowing for CP violation in mixing and in the interference between mixing and decay, we measure the CP-averaged normalized mass difference $x_{CP} = [2.7 \pm 1.6(\text{stat}) \pm 0.4(\text{syst})] \times 10^{-3}$ and the CP-violating parameter $\Delta x = [-0.53 \pm 0.70(\text{stat}) \pm 0.22(\text{syst})] \times 10^{-3}$. The results are consistent with CP symmetry. These determinations are the most precise from a single experiment and, combined with current world-average results, yield the first evidence that the masses of the neutral charm-meson eigenstates differ.

DOI: 10.1103/PhysRevLett.122.231802

Flavor oscillations are transitions between neutral flavored mesons and their corresponding antimesons that follow an oscillating pattern as a function of decay time. In the standard model, these transitions are mediated by weak-interaction amplitudes involving exchanges of virtual $W^\pm$ bosons and heavy quarks. Unknown particles of arbitrarily high mass can contribute as virtual particles in the amplitude, possibly enhancing the average oscillation rate or the difference between the rates of mesons and antimesons. This makes flavor oscillations sensitive to non-standard-model dynamics at large energy scales [1].

Oscillations occur because the mass eigenstates of neutral flavored mesons are linear combinations of the flavor eigenstates. In particular, for charm mesons, one writes $|D_{1,2}\rangle \equiv p|D^0\rangle \pm q|\overline{D}^0\rangle$, where p and q are complex parameters. In the limit of charge-parity (CP) symmetry, and by defining $D_{1(2)}$ as the CP-even (odd) state, the oscillation rate depends only on the dimensionless mixing parameters $x \equiv (m_1 - m_2)c^2/\Gamma$ and $y \equiv (\Gamma_1 - \Gamma_2)/(2\Gamma)$, where $m_{1(2)}$ and $\Gamma_{1(2)}$ are the mass and decay width of the $D_{1(2)}$ state, respectively, and Γ equals $(\Gamma_1 + \Gamma_2)/2$ [2]. If CP symmetry is violated, the oscillation rates for mesons produced as D^0 and $\bar{D}^0$ differ. The difference is generated in the mixing amplitude if $|q/p| \neq 1$ or in the interference between mixing and decay if $\phi_f \equiv \arg(q\overline{A}_f/pA_f) \neq 0$. The amplitude A_f ($\overline{A}_f$) refers to the decay $D^0 \to f$ ($\bar{D}^0 \to f$), where f is a common final state. If CP is conserved in the decay amplitude ($|A_f|^2 = |\overline{A}_f|^2$), the CP-violating phase is independent of the final state $\phi_f \approx \phi = \arg(q/p)$ [3,4].

Current global averages of charm-mixing parameters have large uncertainties and are consistent with CP symmetry, yielding $x = (3.6^{+2.1}_{-1.6}) \times 10^{-3}$, $y = (6.7^{+0.6}_{-1.3}) \times 10^{-3}$, $|q/p| = 0.94^{+0.17}_{-0.07}$, and $\phi = -0.13^{+0.26}_{-0.17}$ [5]. Improving the knowledge of x, which has not been shown to differ significantly from zero, is especially critical because the sensitivity to the small phase ϕ relies predominantly on observables proportional to $x \sin\phi$.

Direct experimental access to charm-mixing parameters is offered by self-conjugate multibody decays, such as $D^0 \to K^0_S\pi^+\pi^-$. Inclusion of charge-conjugate processes is implied unless stated otherwise. A joint fit of the Dalitz-plot and decay-time distributions of these decays allows the identification of a D^0 component that increases as a function of decay time in a sample of candidates produced as $\bar{D}^0$ mesons, and vice versa. This approach is challenging because it requires analyzing the decay-time evolution of signal decays across the Dalitz plot with a detailed amplitude model while accounting for efficiencies, resolutions, and background [6–8]. Model-independent approaches that obviate the need for an amplitude analysis exist [9–11], but they rely on an accurate description of the efficiencies.

This Letter reports on a measurement of charm oscillations in $D^0 \to K^0_S\pi^+\pi^-$ decays based on a novel model-independent approach, called the bin-flip method, which is optimized for the measurement of the parameter x [12]. The method relies on ratios between charm decays reconstructed in similar kinematic and decay-time conditions, thus avoiding the need for an accurate modeling of the efficiency variation across phase space and decay time. We express the $D^0 \to K^0_S\pi^+\pi^-$ dynamics with two invariant masses following the Dalitz formalism [13,14], where $m^2_\pm$ is the squared invariant mass $m^2(K^0_S\pi^\pm)$ for $D^0 \to K^0_S\pi^+\pi^-$

[*]Full author list given at the end of the article.

decays and $m^2(K^0_S\pi^\mp)$ for $\overline{D}{}^0 \to K^0_S\pi^+\pi^-$ decays. We partition the Dalitz plot into disjoint regions ("bins") that preserve nearly constant strong-phase differences $\Delta\delta(m^2_-, m^2_+)$ between the D^0 and $\overline{D}{}^0$ amplitudes within each bin [15]. Two sets of eight bins are formed, and they are organized symmetrically about the principal bisector $m^2_+ = m^2_-$. Bins are labeled with the indices $\pm b$, where $b = 1, \ldots, 8$. Positive indices refer to the (lower) $m^2_+ > m^2_-$ region, where unmixed Cabibbo-favored $D^0 \to K^*(892)^-\pi^+$ decays dominate; negative indices refer to the symmetric (upper) $m^2_+ < m^2_-$ region, which receives a larger contribution from decays following oscillation. The data are further split into bins of decay time, which are indexed with j. For each, we measure the ratio R^+_{bj} (R^-_{bj}) between initially produced D^0 ($\overline{D}{}^0$) mesons in Dalitz bin $-b$ and Dalitz bin b. For small mixing parameters and CP-conserving decay amplitudes, which are good approximations here, the ratios are [12]

$$R^\pm_{bj} \approx \frac{r_b + (1/4)r_b\langle t^2\rangle_j \mathrm{Re}(z^2_{CP} - \Delta z^2) + (1/4)\langle t^2\rangle_j |z_{CP} \pm \Delta z|^2 + \sqrt{r_b}\langle t\rangle_j \mathrm{Re}[X^*_b(z_{CP} \pm \Delta z)]}{1 + (1/4)\langle t^2\rangle_j \mathrm{Re}(z^2_{CP} - \Delta z^2) + r_b(1/4)\langle t^2\rangle_j |z_{CP} \pm \Delta z|^2 + \sqrt{r_b}\langle t\rangle_j \mathrm{Re}[X_b(z_{CP} \pm \Delta z)]}. \quad (1)$$

Here, $\langle t\rangle_j$ ($\langle t^2\rangle_j$) is the average (squared) decay time of unmixed decays in bin j, in units of the D^0 lifetime $\tau = \hbar/\Gamma$ [2]. The parameter r_b is the ratio of signal yields in symmetric Dalitz-plot bins $\mp b$ at $t = 0$, and X_b quantifies the average strong-phase difference in these bins [12]. The z_{CP} and Δz parameters, defined by $z_{CP} \pm \Delta z \equiv -(q/p)^{\pm 1}(y + ix)$, are obtained, along with r_b, from a joint fit of the observed $R^\pm_{bj}$ ratios in which external information on $c_b \equiv \mathrm{Re}(X_b)$ and $s_b \equiv -\mathrm{Im}(X_b)$ [16] is used as a constraint. The results are expressed in terms of the CP-averaged mixing parameters $x_{CP} \equiv -\mathrm{Im}(z_{CP})$ and $y_{CP} \equiv -\mathrm{Re}(z_{CP})$, and of the CP-violating differences $\Delta x \equiv -\mathrm{Im}(\Delta z)$ and $\Delta y \equiv -\mathrm{Re}(\Delta z)$. Conservation of CP symmetry in mixing, or in the interference between mixing and decay, implies $x_{CP} = x$, $y_{CP} = y$, and $\Delta x = \Delta y = 0$.

Samples of $D^0 \to K^0_S\pi^+\pi^-$ decays are reconstructed from proton-proton collisions collected by the LHCb experiment in 2011 and 2012, corresponding to integrated luminosities of 1 and 2 fb^{-1}, respectively. In the 2012 data, both the strong-interaction decay $D^{*+} \to D^0\pi^+$ and the semileptonic b-hadron decay $\overline{B} \to D^0\mu^- X$, where X generically indicates unreconstructed particles, are used to determine whether a D^0 or a $\overline{D}{}^0$ is produced. In the 2011 data, only the $\overline{B} \to D^0\mu^- X$ decays were used because the online-selection efficiency for $D^{*+} \to D^0\pi^+$ decays was low. Throughout this Letter, D^{*+} indicates the $D^*(2010)^+$ meson and a soft pion indicates the pion from its decay.

The LHCb detector is a single-arm forward spectrometer covering the pseudorapidity range $2 < \eta < 5$ equipped with charged-hadron identification detectors, calorimeters, and muon detectors; and it is designed for the study of particles containing b or c quarks [17,18].

The online selection of $D^{*+} \to D^0(\to K^0_S\pi^+\pi^-)\pi^+$ decays (prompt sample) uses criteria on momenta and final-state charged-particle displacements from any proton-proton primary interaction. Offline, we apply criteria consistent with the decay topology on momenta, vertex and track displacements, particle-identification information, and invariant masses of the D^{*+} decay products. Specifically, the mass of the D^0 candidate is required to meet $1.84 < m(K^0_S\pi^+\pi^-) < 1.89$ GeV/c^2, and the difference between the D^{*+} and D^0 candidate masses is required to satisfy $\Delta m < 151.1$ MeV/c^2. The D^0 and soft pion candidates are required to point back to one of the proton-proton interactions (the primary vertex) to suppress signal candidates originating from decays of b hadrons (secondary decays). A kinematic fit constrains the tracks according to the decay topology and the D^{*+} candidate to originate from the primary vertex [19]. In the reconstruction of the Dalitz-plot coordinates, we additionally constrain the K^0_S and D^0 meson masses to the known values [2] to ensure that all candidates populate the kinematically allowed phase space.

The online selection of $\overline{B} \to D^0(\to K^0_S\pi^+\pi^-)\mu^- X$ decays (semileptonic sample) requires at least one displaced high-transverse-momentum muon and a vertex consistent with the decay of a b hadron. Offline, we apply criteria consistent with the decay topology on momenta, vertex and track displacements, particle identifications, and invariant masses of the D^0 decay products. In addition, candidate $D^0\mu^-$ pairs are formed by requiring $2.5 < m(D^0\mu^-) < 6.0$ GeV/c^2 and the corrected mass $\sqrt{m^2(D^0\mu^-) + p^2_\perp(D^0\mu^-)} + p_\perp(D^0\mu^-)$, where the momentum component $p_\perp(D^0\mu^-)$ of the $D^0\mu^-$ system transverse to the $\overline{B}$ flight direction partially compensates for the momentum of unreconstructed decay products, to be smaller than 5.8 GeV/c^2. The $\overline{B}$ flight direction is inferred from the measured positions of the primary and $D^0\mu^-$ vertices. A kinematic fit constrains the D^0 and K^0_S masses to their known values.

In both samples, two categories of signal candidates are used: those with $K^0_S \to \pi^+\pi^-$ candidates reconstructed in the vertex detector (long K^0_S), and those with K^0_S candidates reconstructed after the vertex detector (downstream K^0_S).

About 2% (3%) of the selected D^{*+} ($\overline{B}$) candidates belong to events in which multiple candidates are reconstructed by pairing the same D^0 candidate with different soft pions (muons). For these events, we randomly choose a

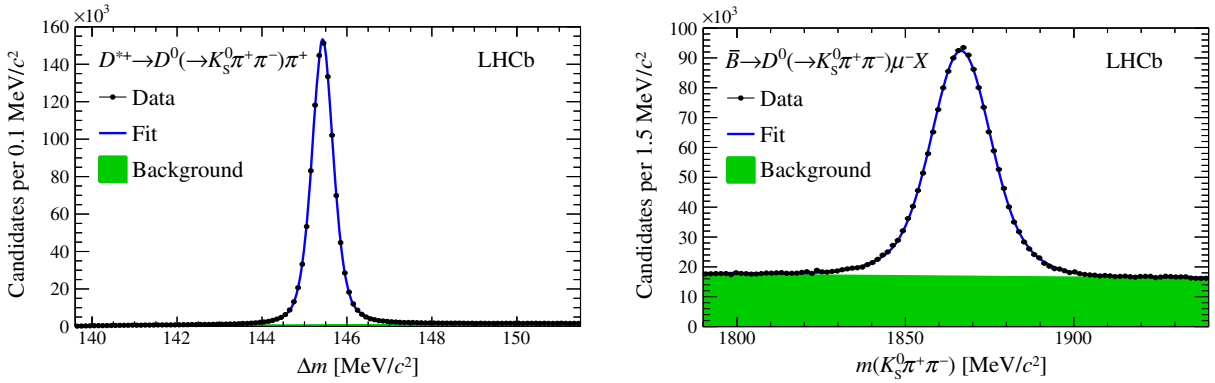

FIG. 1. Distribution of (left) the difference between D^{*+} and D^0 masses for $D^{*+} \to D^0(\to K^0_S\pi^+\pi^-)\pi^+$ candidates and (right) D^0 mass for $\overline{B} \to D^0(\to K^0_S\pi^+\pi^-)\mu^- X$ candidates.

single candidate. We consider the prompt and semileptonic samples independent because their overlap amounts to less than 0.1% of the semileptonic sample size.

Figure 1 shows the Δm and $m(K^0_S\pi^+\pi^-)$ distributions of the prompt and semileptonic samples, respectively. The prompt sample contains 1.3×10^6 signal decays (45% with downstream K^0_S candidates) and a small background dominated by genuine $D^0 \to K^0_S\pi^+\pi^-$ decays associated to random soft pions. Secondary D^{*+} decays contribute approximately 3% to the signal yield, as determined using D^0 candidates not pointing to the primary vertex. The semileptonic sample contains 1.0×10^6 signal decays (66% with downstream K^0_S candidates) and a sizable background dominated by unrelated $K^0_S\pi^+\pi^-$ combinations. Genuine D^0 decays associated with random muons contribute less than 1% to the D^0 yield, as determined from the yield of false $\overline{B}$ candidates formed by associating $D^{*+} \to D^0\pi^+$ with same-sign μ^+ candidates. Contributions from backgrounds due to misreconstructed D^0 decays, such as $D^0 \to K^0_S\pi^+\pi^-\pi^0$ and $D^0 \to K^0_S h^+h^{(\prime)-}$ (where $h^+h^{(\prime)-}$ indicates a pair of light hadrons other than $\pi^+\pi^-$), are negligible.

Simulated [20,21] prompt decays show that the online requirements on displacement and momenta of the D^0 decay products introduce efficiency variations that are correlated between the squared mass of the two final-state pions, $m^2(\pi^+\pi^-)$, and the D^0 decay time. Because $(m^2(\pi^+\pi^-), t)$ correlations can bias the results, we correct for them using data. The smallness of the mixing parameters [5], along with the known $D^0 \to K^0_S\pi^+\pi^-$ decay amplitudes [6–8], rules out any measurable $(m^2(\pi^+\pi^-), t)$ correlation introduced by D^0–$\overline{D}^0$ mixing with current sample sizes. Hence, we ascribe any observed dependence between $m^2(\pi^+\pi^-)$ and t to instrumental effects. We use the background-subtracted $(m^2(\pi^+\pi^-), t)$ distribution to determine the decay-time efficiency, normalized to the average decay-time distribution, as a function of $m^2(\pi^+\pi^-)$. This two-dimensional map is smoothed and used to assign per-candidate weights proportional to the inverse of the relative efficiency at each candidate's $(m^2(\pi^+\pi^-), t)$ coordinates, effectively removing the correlated nonuniformities. The corrections are determined separately for long and downstream K^0_S candidates because they feature different correlations. Figure 2 shows the smoothed $(m^2(\pi^+\pi^-), t)$ map for the sample with downstream K^0_S candidates, where the correlations are more prominent. The 6% of candidates reconstructed with $t < 0.9\tau$ are discarded because the corresponding weights cannot be determined precisely. No $(m^2(\pi^+\pi^-), t)$ correlations are observed in $\overline{B} \to D^0(\to K^0_S\pi^+\pi^-)\mu^- X$ decays.

We divide prompt and semileptonic samples according to the K^0_S category, D^0 meson flavor, Dalitz-plot position, and decay time. In each subsample, we determine the signal yield and—for each decay-time bin—the average decay time and average squared decay time of the signal candidates. Finally, we fit the decay-time dependence of the ratio of the signal yields symmetric with respect to the Dalitz-plot bisector.

We determine the signal yields by fitting the Δm distribution, weighted to correct for the $(m^2(\pi^+\pi^-), t)$ correlations, for the $D^{*+} \to D^0(\to K^0_S\pi^+\pi^-)\pi^+$ candidates and the $m(K^0_S\pi^+\pi^-)$ distribution for the $\overline{B} \to D^0(\to K^0_S\pi^+\pi^-)\mu^- X$ candidates. All components are modeled empirically. The Δm model combines a D^{*+} signal with a smooth

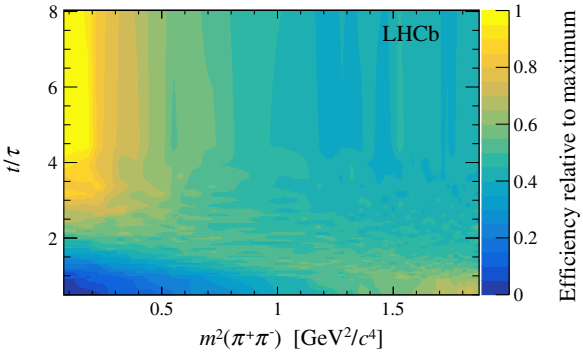

FIG. 2. Smoothed efficiency as a function of $m^2(\pi^+\pi^-)$ and t/τ in $D^{*+} \to D^0(\to K^0_S\pi^+\pi^-)\pi^+$ decays, as determined from the data with downstream K^0_S candidates.

phase-space-like background. The $m(K^0_S\pi^+\pi^-)$ model combines a D^0 signal with a linear background. Signal and background shape parameters are determined independently for long and downstream K^0_S candidates, for D^0 and $\overline{D}^0$ mesons, and in each decay-time and Dalitz-plot bin. The signal model assumes the same parameters for each pair of positive and negative Dalitz-plot bins.

We estimate $\langle t\rangle_j$ and $\langle t^2\rangle_j$ from the background-subtracted t distribution in each decay-time bin j separately for prompt and semileptonic samples, as well as for long and downstream K^0_S candidates. Background is subtracted using weights derived from the mass fits [22] of candidates restricted to the lower half ($m^2_- < m^2_+$) of the Dalitz plot, which is enriched in D^0 mesons that did not undergo oscillations. We neglect the decay-time resolutions, which are typically 0.1τ and 0.25τ for the $D^{*+} \to D^0(\to K^0_S\pi^+\pi^-)\pi^+$ and $\overline{B} \to D^0(\to K^0_S\pi^+\pi^-)\mu^- X$ samples, respectively; and we account for this approximation in the systematic uncertainties.

The mixing parameters are determined by minimizing a least-squares function that compares the decay-time evolution of signal yields (N) observed in Dalitz bins $-b$ and $+b$, along with their uncertainties (σ), with the expected values reported in Eq. (1),

$$\chi^2 \equiv \sum_{\text{pr,sl}}\sum_{l,d}\sum_{+,-}\sum_{b,j}\frac{(N^{\pm}_{-bj} - N^{\pm}_{+bj}R^{\pm}_{+bj})^2}{(\sigma^{\pm}_{-bj})^2 + (\sigma^{\pm}_{+bj}R^{\pm}_{+bj})^2} + \sum_{b,b'}(X^{\text{CLEO}}_b - X_b)(V^{-1}_{\text{CLEO}})_{bb'}(X^{\text{CLEO}}_{b'} - X_{b'}). \quad (2)$$

We fit simultaneously the prompt (pr) and semileptonic (sl) samples, separated between long (l) and downstream (d) K^0_S candidates, as well as between D^0 (+) and $\bar{D}^0$ (−) flavors, across all decay-time bins j and Dalitz-plot bins b. We constrain the parameters X_b to the values X^{CLEO}_b measured by the CLEO collaboration through a Gaussian penalty term that uses the sum V_{CLEO} of the statistical and systematic covariance matrices [16]. In the fit, the parameters r_b are determined independently for each subsample (pr, sl, l, and d) because they are affected by the sample-specific variation of the efficiency over the Dalitz plot [12]. The values of x_{CP}, Δx, and Δy were kept blind until the analysis was finalized.

Figure 3 shows the yield ratios with fit projections overlaid for prompt and semileptonic data. The offsets between semileptonic and prompt data are due to sample-specific efficiency variations across the Dalitz plot; their slopes, due to charm oscillations, are consistent across samples. Table I lists the results. The data are consistent with CP symmetry ($\Delta x = \Delta y = 0$). The precision is dominated by the statistical contribution, which incorporates a subleading component due to the precision of the CLEO measurements.

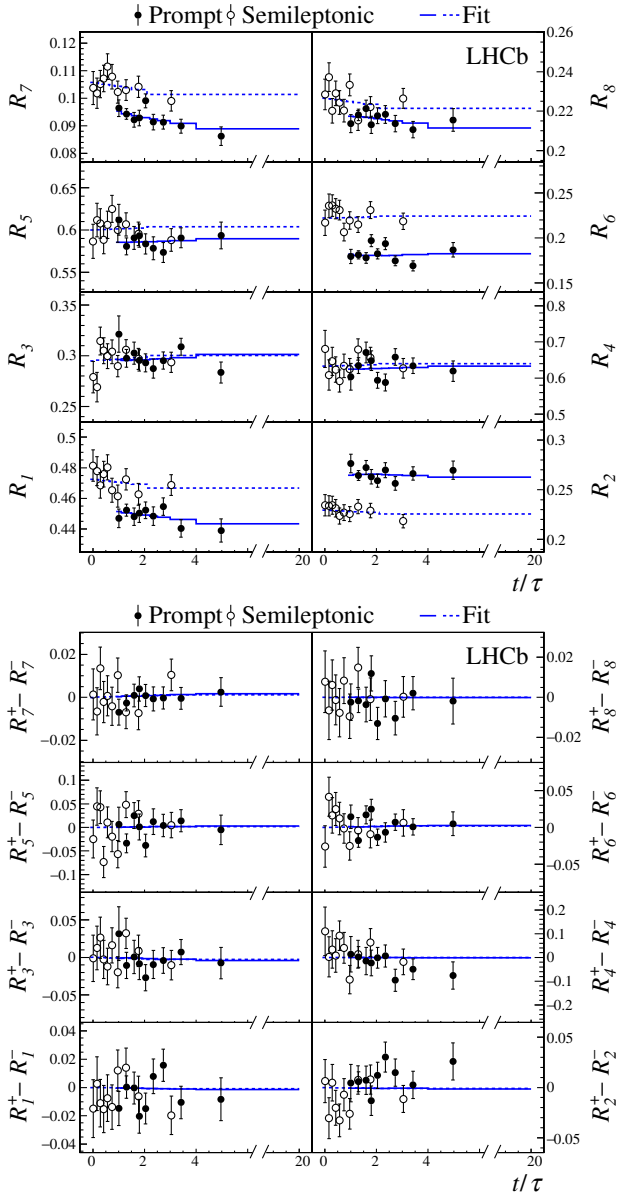

FIG. 3. (Top) CP-averaged yield ratios and (bottom) differences of D^0 and $\overline{D}^0$ yield ratios as functions of t/τ for each Dalitz bin. Prompt (closed points) and semileptonic (open points) data are shown separately. Fit projections over the prompt (solid line) and semileptonic (dashed line) data are overlaid.

The dominant systematic uncertainties on x_{CP} are associated with the 3% contamination from secondary D^{*+} decays in the prompt sample (0.24×10^{-3}) and from the 1% contamination of genuine D^0 mesons associated with random muons in the semileptonic sample (0.34×10^{-3}). Biases due to the neglected decay-time and $m^2_\pm$ resolutions, and the neglected efficiency variations across the decay time and Dalitz plot, constitute the dominant systematic uncertainty on y_{CP} (0.94×10^{-3}). Possible asymmetric nonuniformities with respect to the bisector in the Dalitz plot induced by reconstruction inefficiencies dominate the systematic uncertainty on Δx

TABLE I. Fit results. The first contribution to the uncertainty is statistical, and the second is systematic.

Parameter	Value $[10^{-3}]$	Statistical correlations			Systematic correlations		
		y_{CP}	Δx	Δy	y_{CP}	Δx	Δy
x_{CP}	$2.7 \pm 1.6 \pm 0.4$	−0.17	0.04	−0.02	0.15	0.01	−0.02
y_{CP}	$7.4 \pm 3.6 \pm 1.1$		−0.03	0.01		−0.05	−0.03
Δx	$-0.53 \pm 0.70 \pm 0.22$			−0.13			0.14
Δy	$0.6 \pm 1.6 \pm 0.3$						

(0.22×10^{-3}) and Δy (0.25×10^{-3}). Other minor effects, such as mismodeling in the signal-yield fits or in the determination of the bin-averaged decay times, are also considered. The consistency between results on the prompt and semileptonic sample [15], and on various partitions of the data, supports the robustness of the analysis, including the correction of the $(m^2(\pi^+\pi^-), t)$ correlations.

In summary, we report a measurement of the normalized mass difference between neutral charm-meson eigenstates using the recently proposed bin-flip method. Allowing for CP violation in charm mixing, or in the interference between mixing and decay, we measure the CP-averaged normalized mass difference $x_{CP}=[2.7\pm1.6(\text{stat})\pm0.4(\text{syst})]\times10^{-3}$ and the CP-violating parameter $\Delta x = [-0.53 \pm 0.70(\text{stat}) \pm 0.22(\text{syst})] \times 10^{-3}$. In addition, we report the CP-averaged normalized width difference $y_{CP} = [7.4 \pm 3.6\,(\text{stat}) \pm 1.1\,(\text{syst})] \times 10^{-3}$, along with the corresponding CP-violating parameter $\Delta y = [0.6 \pm 1.6(\text{stat}) \pm 0.3(\text{syst})] \times 10^{-3}$. We use the results to form a likelihood function of x, y, $|q/p|$, and ϕ; and we derive confidence intervals (Table II) using a likelihood-ratio ordering that assumes the observed correlations to be independent of the true parameter values [23]. The resulting determination of the mass difference is the most precise from a single experiment, as are the determinations of the CP-violation parameters. Although our result is consistent with $x = 0$ within two standard deviations, combined with the current global knowledge, it yields $x = (3.9^{+1.1}_{-1.2}) \times 10^{-3}$ [5], strongly contributing to the emerging evidence for a nonzero (positive) mass difference between the neutral charm-meson eigenstates. The global constraints on CP violation in the D^0-$\overline{D}^0$ system are also greatly improved, with precisions on $|q/p|$ and ϕ more than doubled as compared to previous averages [5].

TABLE II. Point estimates and 95.5% confidence-level (C.L.) intervals for the derived parameters. Uncertainties include statistical and systematic contributions.

Parameter	Value	95.5% C.L. interval
x $[10^{-2}]$	$0.27^{+0.17}_{-0.15}$	$[-0.05, 0.60]$
y $[10^{-2}]$	0.74 ± 0.37	$[0.00, 1.50]$
$\lvert q/p \rvert$	$1.05^{+0.22}_{-0.17}$	$[0.55, 2.15]$
ϕ	$-0.09^{+0.11}_{-0.16}$	$[-0.73, 0.29]$

We express our gratitude to our colleagues in the CERN accelerator departments for the excellent performance of the LHC. We thank the technical and administrative staff at the LHCb institutes. We acknowledge support from CERN and from the national agencies: CAPES, CNPq, FAPERJ and FINEP (Brazil); MOST and NSFC (China); CNRS/IN2P3 (France); BMBF, DFG, and MPG (Germany); INFN (Italy); NWO (Netherlands); MNiSW and NCN (Poland); MEN/IFA (Romania); MSHE (Russia); MinECo (Spain); SNSF and SER (Switzerland); NASU (Ukraine); STFC (United Kingdom); NSF (USA). We acknowledge the computing resources that are provided by CERN, IN2P3 (France), KIT and DESY (Germany), INFN (Italy), SURF (Netherlands), PIC (Spain), GridPP (United Kingdom), RRCKI and Yandex LLC (Russia), CSCS (Switzerland), IFIN-HH (Romania), CBPF (Brazil), PL-GRID (Poland), and OSC (USA). We are indebted to the communities behind the multiple open-source software packages on which we depend. Individual groups or members have received support from the AvH Foundation (Germany); EPLANET, Marie Skłodowska-Curie Actions, and ERC (European Union); ANR, Labex P2IO, OCEVU, and Région Auvergne-Rhône-Alpes (France); the Key Research Program of Frontier Sciences of CAS, CAS PIFI, and the Thousand Talents Program (China); RFBR, RSF, and Yandex, LLC (Russia); GVA, XuntaGal, and GENCAT (Spain); the Royal Society and the Leverhulme Trust (United Kingdom); and Laboratory Directed Research and Development program of LANL (USA).

[1] G. Isidori, Y. Nir, and G. Perez, Flavor physics constraints for physics beyond the standard model, Annu. Rev. Nucl. Part. Sci. **60**, 355 (2010).

[2] M. Tanabashi *et al.* (Particle Data Group), Review of particle physics, Phys. Rev. D **98**, 030001 (2018).

[3] D. S. Du, Searching for possible large CP -violation effects in neutral-charm-meson decays, Phys. Rev. D **34**, 3428 (1986).

[4] S. Bergmann, Y. Grossman, Z. Ligeti, Y. Nir, and A. A. Petrov, Lessons from CLEO and FOCUS measurements of D^0–$\overline{D}^0$ mixing parameters, Phys. Lett. B **486**, 418 (2000).

[5] Y. Amhis *et al.* (Heavy Flavor Averaging Group), Averages of b-hadron, c-hadron, and τ-lepton properties as of summer

2016, Eur. Phys. J. C 77, 895 (2017); updated results and plots available at https://hflav.web.cern.ch.
[6] D. M. Asner et al. (CLEO Collaboration), Search for D^0–$\overline{D}^0$ mixing in the Dalitz plot analysis of $D^0 \to K^0_S\pi^+\pi^-$, Phys. Rev. D 72, 012001 (2005).
[7] T. Peng et al. (Belle Collaboration), Measurement of D^0–$\overline{D}^0$ mixing and search for indirect CP violation using $D^0 \to K^0_S\pi^+\pi^-$ decays, Phys. Rev. D 89, 091103 (2014).
[8] P. del Amo Sanchez et al. (BABAR Collaboration), Measurement of D^0–$\overline{D}^0$ Mixing Parameters Using $D^0 \to K^0_S\pi^+\pi^-$ and $D^0 \to K^0_S K^+K^-$ Decays, Phys. Rev. Lett. 105, 081803 (2010).
[9] A. Bondar, A. Poluektov, and V. Vorobiev, Charm mixing in a model-independent analysis of correlated $D^0\overline{D}^0$ decays, Phys. Rev. D 82, 034033 (2010).
[10] C. Thomas and G. Wilkinson, Model-independent D^0–$\overline{D}^0$ mixing and CP violation studies with $D^0 \to K^0_S\pi^+\pi^-$ and $D^0 \to K^0_S K^+K^-$, J. High Energy Phys. 10 (2012) 185.
[11] R. Aaij et al. (LHCb Collaboration), Model-independent measurement of mixing parameters in $D^0 \to K^0_S\pi^+\pi^-$ decays, J. High Energy Phys. 04 (2016) 033.
[12] A. Di Canto, J. G. Ticó, T. Gershon, N. Jurik, M. Martinelli, T. Pilař, S. Stahl, and D. Tonelli, Novel method for measuring charm-mixing parameters using multibody decays, Phys. Rev. D 99, 012007 (2019).
[13] R. H. Dalitz, On the analysis of τ-meson data and the nature of the τ-meson, Philos. Mag. Ser. 7, 44, 1068 (1953).
[14] E. Fabri, A study of τ-meson decay, Nuovo Cimento 11, 479 (1954).
[15] See Supplemental Material at http://link.aps.org/supplemental/10.1103/PhysRevLett.122.231802 for figures showing the Dalitz-plot distribution of the data and the Dalitz-plot binning scheme used in the analysis; and for tables with results obtained by fitting independently the prompt and semileptonic data samples.
[16] J. Libby et al. (CLEO Collaboration), Model-independent determination of the strong-phase difference between D^0 and $\overline{D}^0 \to K^0_{S,L}h^+h^-$ ($h = \pi$, K) and its impact on the measurement of the CKM angle γ/ϕ_3, Phys. Rev. D 82, 112006 (2010).
[17] A. A. Alves, Jr. et al. (LHCb Collaboration), The LHCb detector at the LHC, J. Instrum. 3, S08005 (2008).
[18] R. Aaij et al. (LHCb Collaboration), LHCb detector performance, Int. J. Mod. Phys. A 30, 1530022 (2015).
[19] W. D. Hulsbergen, Decay chain fitting with a Kalman filter, Nucl. Instrum. Methods Phys. Res., Sect. A 552, 566 (2005).
[20] M. Clemencic, G. Corti, S. Easo, C. R. Jones, S. Miglioranzi, M. Pappagallo, and P. Robbe, The LHCb simulation application, Gauss: Design, evolution and experience, J. Phys. Conf. Ser. 331, 032023 (2011).
[21] I. Belyaev et al., Handling of the generation of primary events in Gauss, the LHCb simulation framework, J. Phys. Conf. Ser. 331, 032047 (2011).
[22] M. Pivk and F. R. Le Diberder, sPlot: A statistical tool to unfold data distributions, Nucl. Instrum. Methods Phys. Res., Sect. A 555, 356 (2005).
[23] R. Aaij et al. (LHCb Collaboration), Measurement of the CKM angle γ from a combination of $B^\pm \to Dh^\pm$ analyses, Phys. Lett. B 726, 151 (2013).

R. Aaij,[29] C. Abellán Beteta,[46] B. Adeva,[43] M. Adinolfi,[50] C. A. Aidala,[77] Z. Ajaltouni,[7] S. Akar,[61] P. Albicocco,[20] J. Albrecht,[12] F. Alessio,[44] M. Alexander,[55] A. Alfonso Albero,[42] G. Alkhazov,[41] P. Alvarez Cartelle,[57] A. A. Alves Jr.,[43] S. Amato,[2] Y. Amhis,[9] L. An,[19] L. Anderlini,[19] G. Andreassi,[45] M. Andreotti,[18] J. E. Andrews,[62] F. Archilli,[29] J. Arnau Romeu,[8] A. Artamonov,[40] M. Artuso,[63] K. Arzymatov,[38] E. Aslanides,[8] M. Atzeni,[46] B. Audurier,[24] S. Bachmann,[14] J. J. Back,[52] S. Baker,[57] V. Balagura,[9,b] W. Baldini,[18,44] A. Baranov,[38] R. J. Barlow,[58] G. C. Barrand,[9] S. Barsuk,[9] W. Barter,[57] M. Bartolini,[21] F. Baryshnikov,[73] V. Batozskaya,[33] B. Batsukh,[63] A. Battig,[12] V. Battista,[45] A. Bay,[45] F. Bedeschi,[26] I. Bediaga,[1] A. Beiter,[63] L. J. Bel,[29] S. Belin,[24] N. Beliy,[4] V. Bellee,[45] N. Belloli,[22,c] K. Belous,[40] I. Belyaev,[35] G. Bencivenni,[20] E. Ben-Haim,[10] S. Benson,[29] S. Beranek,[11] A. Berezhnoy,[36] R. Bernet,[46] D. Berninghoff,[14] E. Bertholet,[10] A. Bertolin,[25] C. Betancourt,[46] F. Betti,[17,d] M. O. Bettler,[51] Ia. Bezshyiko,[46] S. Bhasin,[50] J. Bhom,[31] M. S. Bieker,[12] S. Bifani,[49] P. Billoir,[10] A. Birnkraut,[12] A. Bizzeti,[19,e] M. Bjørn,[59] M. P. Blago,[44] T. Blake,[52] F. Blanc,[45] S. Blusk,[63] D. Bobulska,[55] V. Bocci,[28] O. Boente Garcia,[43] T. Boettcher,[60] A. Bondar,[39,f] N. Bondar,[41] S. Borghi,[58,44] M. Borisyak,[38] M. Borsato,[14] M. Boubdir,[11] T. J. V. Bowcock,[56] C. Bozzi,[18,44] S. Braun,[14] M. Brodski,[44] J. Brodzicka,[31] A. Brossa Gonzalo,[52] D. Brundu,[24,44] E. Buchanan,[50] A. Buonaura,[46] C. Burr,[58] A. Bursche,[24] J. Buytaert,[44] W. Byczynski,[44] S. Cadeddu,[24] H. Cai,[67] R. Calabrese,[18,g] R. Calladine,[49] M. Calvi,[22,c] M. Calvo Gomez,[42,h] A. Camboni,[42,h] P. Campana,[20] D. H. Campora Perez,[44] L. Capriotti,[17,d] A. Carbone,[17,d] G. Carboni,[27] R. Cardinale,[21] A. Cardini,[24] P. Carniti,[22,c] K. Carvalho Akiba,[2] G. Casse,[56] M. Cattaneo,[44] G. Cavallero,[21] R. Cenci,[26,i] D. Chamont,[9] M. G. Chapman,[50] M. Charles,[10,44] Ph. Charpentier,[44] G. Chatzikonstantinidis,[49] M. Chefdeville,[6] V. Chekalina,[38] C. Chen,[3] S. Chen,[24] S.-G. Chitic,[44] V. Chobanova,[43] M. Chrzaszcz,[44] A. Chubykin,[41] P. Ciambrone,[20] X. Cid Vidal,[43] G. Ciezarek,[44] F. Cindolo,[17] P. E. L. Clarke,[54] M. Clemencic,[44] H. V. Cliff,[51] J. Closier,[44] V. Coco,[44] J. A. B. Coelho,[9] J. Cogan,[8] E. Cogneras,[7] L. Cojocariu,[34] P. Collins,[44] T. Colombo,[44] A. Comerma-Montells,[14] A. Contu,[24] G. Coombs,[44]

S. Coquereau,[42] G. Corti,[44] C. M. Costa Sobral,[52] B. Couturier,[44] G. A. Cowan,[54] D. C. Craik,[60] A. Crocombe,[52] M. Cruz Torres,[1] R. Currie,[54] C. L. Da Silva,[78] E. Dall'Occo,[29] J. Dalseno,[43,j] C. D'Ambrosio,[44] A. Danilina,[35] P. d'Argent,[14] A. Davis,[58] O. De Aguiar Francisco,[44] K. De Bruyn,[44] S. De Capua,[58] M. De Cian,[45] J. M. De Miranda,[1] L. De Paula,[2] M. De Serio,[16,k] P. De Simone,[20] J. A. de Vries,[29] C. T. Dean,[55] W. Dean,[77] D. Decamp,[6] L. Del Buono,[10] B. Delaney,[51] H.-P. Dembinski,[13] M. Demmer,[12] A. Dendek,[32] D. Derkach,[74] O. Deschamps,[7] F. Desse,[9] F. Dettori,[24] B. Dey,[68] A. Di Canto,[44] P. Di Nezza,[20] S. Didenko,[73] H. Dijkstra,[44] F. Dordei,[24] M. Dorigo,[44,l] A. C. dos Reis,[1] A. Dosil Suárez,[43] L. Douglas,[55] A. Dovbnya,[47] K. Dreimanis,[56] L. Dufour,[44] G. Dujany,[10] P. Durante,[44] J. M. Durham,[78] D. Dutta,[58] R. Dzhelyadin,[40,a] M. Dziewiecki,[14] A. Dziurda,[31] A. Dzyuba,[41] S. Easo,[53] U. Egede,[57] V. Egorychev,[35] S. Eidelman,[39,f] S. Eisenhardt,[54] U. Eitschberger,[12] R. Ekelhof,[12] L. Eklund,[55] S. Ely,[63] A. Ene,[34] S. Escher,[11] S. Esen,[29] T. Evans,[61] A. Falabella,[17] C. Färber,[44] N. Farley,[49] S. Farry,[56] D. Fazzini,[22,c] M. Féo,[44] P. Fernandez Declara,[44] A. Fernandez Prieto,[43] F. Ferrari,[17,d] L. Ferreira Lopes,[45] F. Ferreira Rodrigues,[2] S. Ferreres Sole,[29] M. Ferro-Luzzi,[44] S. Filippov,[37] R. A. Fini,[16] M. Fiorini,[18,g] M. Firlej,[32] C. Fitzpatrick,[45] T. Fiutowski,[32] F. Fleuret,[9,b] M. Fontana,[44] F. Fontanelli,[21,m] R. Forty,[44] V. Franco Lima,[56] M. Frank,[44] C. Frei,[44] J. Fu,[23,n] W. Funk,[44] E. Gabriel,[54] A. Gallas Torreira,[43] D. Galli,[17,d] S. Gallorini,[25] S. Gambetta,[54] Y. Gan,[3] M. Gandelman,[2] P. Gandini,[23] Y. Gao,[3] L. M. Garcia Martin,[76] J. García Pardiñas,[46] B. Garcia Plana,[43] J. Garra Tico,[51] L. Garrido,[42] D. Gascon,[42] C. Gaspar,[44] G. Gazzoni,[7] D. Gerick,[14] E. Gersabeck,[58] M. Gersabeck,[58] T. Gershon,[52] D. Gerstel,[8] Ph. Ghez,[6] V. Gibson,[51] O. G. Girard,[45] P. Gironella Gironell,[42] L. Giubega,[34] K. Gizdov,[54] V. V. Gligorov,[10] C. Göbel,[65] D. Golubkov,[35] A. Golutvin,[57,73] A. Gomes,[1,o] I. V. Gorelov,[36] C. Gotti,[22,c] E. Govorkova,[29] J. P. Grabowski,[14] R. Graciani Diaz,[42] L. A. Granado Cardoso,[44] E. Graugés,[42] E. Graverini,[46] G. Graziani,[19] A. Grecu,[34] R. Greim,[29] P. Griffith,[24] L. Grillo,[58] L. Gruber,[44] B. R. Gruberg Cazon,[59] C. Gu,[3] E. Gushchin,[37] A. Guth,[11] Yu. Guz,[40,44] T. Gys,[44] T. Hadavizadeh,[59] C. Hadjivasiliou,[7] G. Haefeli,[45] C. Haen,[44] S. C. Haines,[51] B. Hamilton,[62] X. Han,[14] T. H. Hancock,[59] S. Hansmann-Menzemer,[14] N. Harnew,[59] T. Harrison,[56] C. Hasse,[44] M. Hatch,[44] J. He,[4] M. Hecker,[57] K. Heinicke,[12] A. Heister,[12] K. Hennessy,[56] L. Henry,[76] M. Heß,[70] J. Heuel,[11] A. Hicheur,[64] R. Hidalgo Charman,[58] D. Hill,[59] M. Hilton,[58] P. H. Hopchev,[45] J. Hu,[14] W. Hu,[68] W. Huang,[4] Z. C. Huard,[61] W. Hulsbergen,[29] T. Humair,[57] M. Hushchyn,[74] D. Hutchcroft,[56] D. Hynds,[29] P. Ibis,[12] M. Idzik,[32] P. Ilten,[49] A. Inglessi,[41] A. Inyakin,[40] K. Ivshin,[41] R. Jacobsson,[44] S. Jakobsen,[44] J. Jalocha,[59] E. Jans,[29] B. K. Jashal,[76] A. Jawahery,[62] F. Jiang,[3] M. John,[59] D. Johnson,[44] C. R. Jones,[51] C. Joram,[44] B. Jost,[44] N. Jurik,[59] S. Kandybei,[47] M. Karacson,[44] J. M. Kariuki,[50] S. Karodia,[55] N. Kazeev,[74] M. Kecke,[14] F. Keizer,[51] M. Kelsey,[63] M. Kenzie,[51] T. Ketel,[30] B. Khanji,[44] A. Kharisova,[75] C. Khurewathanakul,[45] K. E. Kim,[63] T. Kirn,[11] V. S. Kirsebom,[45] S. Klaver,[20] K. Klimaszewski,[33] S. Koliiev,[48] M. Kolpin,[14] R. Kopecna,[14] P. Koppenburg,[29] I. Kostiuk,[29,48] S. Kotriakhova,[41] M. Kozeiha,[7] L. Kravchuk,[37] M. Kreps,[52] F. Kress,[57] S. Kretzschmar,[11] P. Krokovny,[39,f] W. Krupa,[32] W. Krzemien,[33] W. Kucewicz,[31,p] M. Kucharczyk,[31] V. Kudryavtsev,[39,f] A. K. Kuonen,[45] T. Kvaratskheliya,[35] D. Lacarrere,[44] G. Lafferty,[58] A. Lai,[24] D. Lancierini,[46] G. Lanfranchi,[20] C. Langenbruch,[11] T. Latham,[52] C. Lazzeroni,[49] R. Le Gac,[8] R. Lefèvre,[7] A. Leflat,[36] F. Lemaitre,[44] O. Leroy,[8] T. Lesiak,[31] B. Leverington,[14] H. Li,[66] P.-R. Li,[4,q] Y. Li,[5] Z. Li,[63] X. Liang,[63] T. Likhomanenko,[72] R. Lindner,[44] F. Lionetto,[46] V. Lisovskyi,[9] G. Liu,[66] X. Liu,[3] D. Loh,[52] A. Loi,[24] I. Longstaff,[55] J. H. Lopes,[2] G. Loustau,[46] G. H. Lovell,[51] D. Lucchesi,[25,r] M. Lucio Martinez,[43] Y. Luo,[3] A. Lupato,[25] E. Luppi,[18,g] O. Lupton,[52] A. Lusiani,[26] X. Lyu,[4] F. Machefert,[9] F. Maciuc,[34] V. Macko,[45] P. Mackowiak,[12] S. Maddrell-Mander,[50] O. Maev,[41,44] K. Maguire,[58] D. Maisuzenko,[41] M. W. Majewski,[32] S. Malde,[59] B. Malecki,[44] A. Malinin,[72] T. Maltsev,[39,f] H. Malygina,[14] G. Manca,[24,s] G. Mancinelli,[8] D. Marangotto,[23,n] J. Maratas,[7,t] J. F. Marchand,[6] U. Marconi,[17] C. Marin Benito,[9] M. Marinangeli,[45] P. Marino,[45] J. Marks,[14] P. J. Marshall,[56] G. Martellotti,[28] M. Martinelli,[44] D. Martinez Santos,[43] F. Martinez Vidal,[76] A. Massafferri,[1] M. Materok,[11] R. Matev,[44] A. Mathad,[46] Z. Mathe,[44] V. Matiunin,[35] C. Matteuzzi,[22] K. R. Mattioli,[77] A. Mauri,[46] E. Maurice,[9,b] B. Maurin,[45] M. McCann,[57,44] A. McNab,[58] R. McNulty,[15] J. V. Mead,[56] B. Meadows,[61] C. Meaux,[8] N. Meinert,[70] D. Melnychuk,[33] M. Merk,[29] A. Merli,[23,n] E. Michielin,[25] D. A. Milanes,[69] E. Millard,[52] M.-N. Minard,[6] L. Minzoni,[18,g] D. S. Mitzel,[14] A. Mödden,[12] A. Mogini,[10] R. D. Moise,[57] T. Mombächer,[12] I. A. Monroy,[69] S. Monteil,[7] M. Morandin,[25] G. Morello,[20] M. J. Morello,[26,u] J. Moron,[32] A. B. Morris,[8] R. Mountain,[63] F. Muheim,[54] M. Mukherjee,[68] M. Mulder,[29] D. Müller,[44] J. Müller,[12] K. Müller,[46] V. Müller,[12] C. H. Murphy,[59] D. Murray,[58] P. Naik,[50] T. Nakada,[45] R. Nandakumar,[53] A. Nandi,[59] T. Nanut,[45] I. Nasteva,[2] M. Needham,[54] N. Neri,[23,n] S. Neubert,[14] N. Neufeld,[44] R. Newcombe,[57] T. D. Nguyen,[45] C. Nguyen-Mau,[45,v] S. Nieswand,[11] R. Niet,[12] N. Nikitin,[36] N. S. Nolte,[44] A. Oblakowska-Mucha,[32] V. Obraztsov,[40] S. Ogilvy,[55] D. P. O'Hanlon,[17] R. Oldeman,[24,s] C. J. G. Onderwater,[71] J. D. Osborn,[77] A. Ossowska,[31] J. M. Otalora Goicochea,[2] T. Ovsiannikova,[35] P. Owen,[46] A. Oyanguren,[76] P. R. Pais,[45]

T. Pajero,[26,u] A. Palano,[16] M. Palutan,[20] G. Panshin,[75] A. Papanestis,[53] M. Pappagallo,[54] L. L. Pappalardo,[18,g] W. Parker,[62] C. Parkes,[58,44] G. Passaleva,[19,44] A. Pastore,[16] M. Patel,[57] C. Patrignani,[17,d] A. Pearce,[44] A. Pellegrino,[29] G. Penso,[28] M. Pepe Altarelli,[44] S. Perazzini,[44] D. Pereima,[35] P. Perret,[7] L. Pescatore,[45] K. Petridis,[50] A. Petrolini,[21,m] A. Petrov,[72] S. Petrucci,[54] M. Petruzzo,[23,n] B. Pietrzyk,[6] G. Pietrzyk,[45] M. Pikies,[31] M. Pili,[59] D. Pinci,[28] J. Pinzino,[44] F. Pisani,[44] A. Piucci,[14] V. Placinta,[34] S. Playfer,[54] J. Plews,[49] M. Plo Casasus,[43] F. Polci,[10] M. Poli Lener,[20] M. Poliakova,[63] A. Poluektov,[8] N. Polukhina,[73,w] I. Polyakov,[63] E. Polycarpo,[2] G. J. Pomery,[50] S. Ponce,[44] A. Popov,[40] D. Popov,[49,13] S. Poslavskii,[40] E. Price,[50] C. Prouve,[43] V. Pugatch,[48] A. Puig Navarro,[46] H. Pullen,[59] G. Punzi,[26,i] W. Qian,[4] J. Qin,[4] R. Quagliani,[10] B. Quintana,[7] N. V. Raab,[15] B. Rachwal,[32] J. H. Rademacker,[50] M. Rama,[26] M. Ramos Pernas,[43] M. S. Rangel,[2] F. Ratnikov,[38,74] G. Raven,[30] M. Ravonel Salzgeber,[44] M. Reboud,[6] F. Redi,[45] S. Reichert,[12] F. Reiss,[10] C. Remon Alepuz,[76] Z. Ren,[3] V. Renaudin,[59] S. Ricciardi,[53] S. Richards,[50] K. Rinnert,[56] P. Robbe,[9] A. Robert,[10] A. B. Rodrigues,[45] E. Rodrigues,[61] J. A. Rodriguez Lopez,[69] M. Roehrken,[44] S. Roiser,[44] A. Rollings,[59] V. Romanovskiy,[40] A. Romero Vidal,[43] J. D. Roth,[77] M. Rotondo,[20] M. S. Rudolph,[63] T. Ruf,[44] J. Ruiz Vidal,[76] J. J. Saborido Silva,[43] N. Sagidova,[41] B. Saitta,[24,s] V. Salustino Guimaraes,[65] C. Sanchez Gras,[29] C. Sanchez Mayordomo,[76] B. Sanmartin Sedes,[43] R. Santacesaria,[28] C. Santamarina Rios,[43] M. Santimaria,[20,44] E. Santovetti,[27,x] G. Sarpis,[58] A. Sarti,[20,y] C. Satriano,[28,z] A. Satta,[27] M. Saur,[4] D. Savrina,[35,36] S. Schael,[11] M. Schellenberg,[12] M. Schiller,[55] H. Schindler,[44] M. Schmelling,[13] T. Schmelzer,[12] B. Schmidt,[44] O. Schneider,[45] A. Schopper,[44] H. F. Schreiner,[61] M. Schubiger,[45] S. Schulte,[45] M. H. Schune,[9] R. Schwemmer,[44] B. Sciascia,[20] A. Sciubba,[28,y] A. Semennikov,[35] E. S. Sepulveda,[10] A. Sergi,[49,44] N. Serra,[46] J. Serrano,[8] L. Sestini,[25] A. Seuthe,[12] P. Seyfert,[44] M. Shapkin,[40] T. Shears,[56] L. Shekhtman,[39,f] V. Shevchenko,[72] E. Shmanin,[73] B. G. Siddi,[18] R. Silva Coutinho,[46] L. Silva de Oliveira,[2] G. Simi,[25,r] S. Simone,[16,k] I. Skiba,[18] N. Skidmore,[14] T. Skwarnicki,[63] M. W. Slater,[49] J. G. Smeaton,[51] E. Smith,[11] I. T. Smith,[54] M. Smith,[57] M. Soares,[17] l. Soares Lavra,[1] M. D. Sokoloff,[61] F. J. P. Soler,[55] B. Souza De Paula,[2] B. Spaan,[12] E. Spadaro Norella,[23,n] P. Spradlin,[55] F. Stagni,[44] M. Stahl,[14] S. Stahl,[44] P. Stefko,[45] S. Stefkova,[57] O. Steinkamp,[46] S. Stemmle,[14] O. Stenyakin,[40] M. Stepanova,[41] H. Stevens,[12] A. Stocchi,[9] S. Stone,[63] S. Stracka,[26] M. E. Stramaglia,[45] M. Straticiuc,[34] U. Straumann,[46] S. Strokov,[75] J. Sun,[3] L. Sun,[67] Y. Sun,[62] K. Swientek,[32] A. Szabelski,[33] T. Szumlak,[32] M. Szymanski,[4] Z. Tang,[3] T. Tekampe,[12] G. Tellarini,[18] F. Teubert,[44] E. Thomas,[44] M. J. Tilley,[57] V. Tisserand,[7] S. T'Jampens,[6] M. Tobin,[5] S. Tolk,[44] L. Tomassetti,[18,g] D. Tonelli,[26] D. Y. Tou,[10] R. Tourinho Jadallah Aoude,[1] E. Tournefier,[6] M. Traill,[55] M. T. Tran,[45] A. Trisovic,[51] A. Tsaregorodtsev,[8] G. Tuci,[26,44,i] A. Tully,[51] N. Tuning,[29] A. Ukleja,[33] A. Usachov,[9] A. Ustyuzhanin,[38,74] U. Uwer,[14] A. Vagner,[75] V. Vagnoni,[17] A. Valassi,[44] S. Valat,[44] G. Valenti,[17] M. van Beuzekom,[29] E. van Herwijnen,[44] C. B. Van Hulse,[15] J. van Tilburg,[29] M. van Veghel,[29] R. Vazquez Gomez,[44] P. Vazquez Regueiro,[43] C. Vázquez Sierra,[29] S. Vecchi,[18] J. J. Velthuis,[50] M. Veltri,[19,aa] A. Venkateswaran,[63] M. Vernet,[7] M. Veronesi,[29] M. Vesterinen,[52] J. V. Viana Barbosa,[44] D. Vieira,[4] M. Vieites Diaz,[43] H. Viemann,[70] X. Vilasis-Cardona,[42,h] A. Vitkovskiy,[29] M. Vitti,[51] V. Volkov,[36] A. Vollhardt,[46] D. Vom Bruch,[10] B. Voneki,[44] A. Vorobyev,[41] V. Vorobyev,[39,f] N. Voropaev,[41] R. Waldi,[70] J. Walsh,[26] J. Wang,[5] M. Wang,[3] Y. Wang,[68] Z. Wang,[46] D. R. Ward,[51] H. M. Wark,[56] N. K. Watson,[49] D. Websdale,[57] A. Weiden,[46] C. Weisser,[60] M. Whitehead,[11] G. Wilkinson,[59] M. Wilkinson,[63] I. Williams,[51] M. Williams,[60] M. R. J. Williams,[58] T. Williams,[49] F. F. Wilson,[53] M. Winn,[9] W. Wislicki,[33] M. Witek,[31] G. Wormser,[9] S. A. Wotton,[51] K. Wyllie,[44] D. Xiao,[68] Y. Xie,[68] H. Xing,[66] A. Xu,[3] M. Xu,[68] Q. Xu,[4] Z. Xu,[6] Z. Xu,[3] Z. Yang,[3] Z. Yang,[62] Y. Yao,[63] L. E. Yeomans,[56] H. Yin,[68] J. Yu,[68,bb] X. Yuan,[63] O. Yushchenko,[40] K. A. Zarebski,[49] M. Zavertyaev,[13,w] M. Zeng,[3] D. Zhang,[68] L. Zhang,[3] W. C. Zhang,[3,cc] Y. Zhang,[44] A. Zhelezov,[14] Y. Zheng,[4] X. Zhu,[3] V. Zhukov,[11,36] J. B. Zonneveld,[54] and S. Zucchelli[17,d]

(LHCb Collaboration)

[1]*Centro Brasileiro de Pesquisas Físicas (CBPF), Rio de Janeiro, Brazil*
[2]*Universidade Federal do Rio de Janeiro (UFRJ), Rio de Janeiro, Brazil*
[3]*Center for High Energy Physics, Tsinghua University, Beijing, China*
[4]*University of Chinese Academy of Sciences, Beijing, China*
[5]*Institute Of High Energy Physics (ihep), Beijing, China*
[6]*Univ. Grenoble Alpes, Univ. Savoie Mont Blanc, CNRS, IN2P3-LAPP, Annecy, France*
[7]*Université Clermont Auvergne, CNRS/IN2P3, LPC, Clermont-Ferrand, France*
[8]*Aix Marseille Univ, CNRS/IN2P3, CPPM, Marseille, France*

[9]LAL, Univ. Paris-Sud, CNRS/IN2P3, Université Paris-Saclay, Orsay, France
[10]LPNHE, Sorbonne Université, Paris Diderot Sorbonne Paris Cité, CNRS/IN2P3, Paris, France
[11]I. Physikalisches Institut, RWTH Aachen University, Aachen, Germany
[12]Fakultät Physik, Technische Universität Dortmund, Dortmund, Germany
[13]Max-Planck-Institut für Kernphysik (MPIK), Heidelberg, Germany
[14]Physikalisches Institut, Ruprecht-Karls-Universität Heidelberg, Heidelberg, Germany
[15]School of Physics, University College Dublin, Dublin, Ireland
[16]INFN Sezione di Bari, Bari, Italy
[17]INFN Sezione di Bologna, Bologna, Italy
[18]INFN Sezione di Ferrara, Ferrara, Italy
[19]INFN Sezione di Firenze, Firenze, Italy
[20]INFN Laboratori Nazionali di Frascati, Frascati, Italy
[21]INFN Sezione di Genova, Genova, Italy
[22]INFN Sezione di Milano-Bicocca, Milano, Italy
[23]INFN Sezione di Milano, Milano, Italy
[24]INFN Sezione di Cagliari, Monserrato, Italy
[25]INFN Sezione di Padova, Padova, Italy
[26]INFN Sezione di Pisa, Pisa, Italy
[27]INFN Sezione di Roma Tor Vergata, Roma, Italy
[28]INFN Sezione di Roma La Sapienza, Roma, Italy
[29]Nikhef National Institute for Subatomic Physics, Amsterdam, Netherlands
[30]Nikhef National Institute for Subatomic Physics and VU University Amsterdam, Amsterdam, Netherlands
[31]Henryk Niewodniczanski Institute of Nuclear Physics Polish Academy of Sciences, Kraków, Poland
[32]AGH—University of Science and Technology, Faculty of Physics and Applied Computer Science, Kraków, Poland
[33]National Center for Nuclear Research (NCBJ), Warsaw, Poland
[34]Horia Hulubei National Institute of Physics and Nuclear Engineering, Bucharest-Magurele, Romania
[35]Institute of Theoretical and Experimental Physics (ITEP), Moscow, Russia
[36]Institute of Nuclear Physics, Moscow State University (SINP MSU), Moscow, Russia
[37]Institute for Nuclear Research of the Russian Academy of Sciences (INR RAS), Moscow, Russia
[38]Yandex School of Data Analysis, Moscow, Russia
[39]Budker Institute of Nuclear Physics (SB RAS), Novosibirsk, Russia
[40]Institute for High Energy Physics (IHEP), Protvino, Russia
[41]Konstantinov Nuclear Physics Institute of National Research Centre "Kurchatov Institute", PNPI, St.Petersburg, Russia
[42]ICCUB, Universitat de Barcelona, Barcelona, Spain
[43]Instituto Galego de Física de Altas Enerxías (IGFAE), Universidade de Santiago de Compostela, Santiago de Compostela, Spain
[44]European Organization for Nuclear Research (CERN), Geneva, Switzerland
[45]Institute of Physics, Ecole Polytechnique Fédérale de Lausanne (EPFL), Lausanne, Switzerland
[46]Physik-Institut, Universität Zürich, Zürich, Switzerland
[47]NSC Kharkiv Institute of Physics and Technology (NSC KIPT), Kharkiv, Ukraine
[48]Institute for Nuclear Research of the National Academy of Sciences (KINR), Kyiv, Ukraine
[49]University of Birmingham, Birmingham, United Kingdom
[50]H.H. Wills Physics Laboratory, University of Bristol, Bristol, United Kingdom
[51]Cavendish Laboratory, University of Cambridge, Cambridge, United Kingdom
[52]Department of Physics, University of Warwick, Coventry, United Kingdom
[53]STFC Rutherford Appleton Laboratory, Didcot, United Kingdom
[54]School of Physics and Astronomy, University of Edinburgh, Edinburgh, United Kingdom
[55]School of Physics and Astronomy, University of Glasgow, Glasgow, United Kingdom
[56]Oliver Lodge Laboratory, University of Liverpool, Liverpool, United Kingdom
[57]Imperial College London, London, United Kingdom
[58]School of Physics and Astronomy, University of Manchester, Manchester, United Kingdom
[59]Department of Physics, University of Oxford, Oxford, United Kingdom
[60]Massachusetts Institute of Technology, Cambridge, Massachusetts, USA
[61]University of Cincinnati, Cincinnati, Ohio, USA
[62]University of Maryland, College Park, Maryland, USA
[63]Syracuse University, Syracuse, New York, USA
[64]Laboratory of Mathematical and Subatomic Physics, Constantine, Algeria
[associated with Universidade Federal do Rio de Janeiro (UFRJ), Rio de Janeiro, Brazil]
[65]Pontifícia Universidade Católica do Rio de Janeiro (PUC-Rio), Rio de Janeiro, Brazil
[associated with Universidade Federal do Rio de Janeiro (UFRJ), Rio de Janeiro, Brazil]

[66]South China Normal University, Guangzhou, China (associated with Center for High Energy Physics, Tsinghua University, Beijing, China)
[67]School of Physics and Technology, Wuhan University, Wuhan, China (associated with Center for High Energy Physics, Tsinghua University, Beijing, China)
[68]Institute of Particle Physics, Central China Normal University, Wuhan, Hubei, China (associated with Center for High Energy Physics, Tsinghua University, Beijing, China)
[69]Departamento de Fisica, Universidad Nacional de Colombia, Bogota, Colombia (associated with LPNHE, Sorbonne Université, Paris Diderot Sorbonne Paris Cité, CNRS/IN2P3, Paris, France)
[70]Institut für Physik, Universität Rostock, Rostock, Germany (associated with Physikalisches Institut, Ruprecht-Karls-Universität Heidelberg, Heidelberg, Germany)
[71]Van Swinderen Institute, University of Groningen, Groningen, Netherlands (associated with Nikhef National Institute for Subatomic Physics, Amsterdam, Netherlands)
[72]National Research Centre Kurchatov Institute, Moscow, Russia [associated with Institute of Theoretical and Experimental Physics (ITEP), Moscow, Russia]
[73]National University of Science and Technology "MISIS", Moscow, Russia [associated with Institute of Theoretical and Experimental Physics (ITEP), Moscow, Russia]
[74]National Research University Higher School of Economics, Moscow, Russia (associated with Yandex School of Data Analysis, Moscow, Russia)
[75]National Research Tomsk Polytechnic University, Tomsk, Russia [associated with Institute of Theoretical and Experimental Physics (ITEP), Moscow, Russia]
[76]Instituto de Fisica Corpuscular, Centro Mixto Universidad de Valencia—CSIC, Valencia, Spain (associated with ICCUB, Universitat de Barcelona, Barcelona, Spain)
[77]University of Michigan, Ann Arbor, USA (associated with Syracuse University, Syracuse, New York, USA)
[78]Los Alamos National Laboratory (LANL), Los Alamos, USA (associated with Syracuse University, Syracuse, New York, USA)

[a]Deceased.
[b]Also at Laboratoire Leprince-Ringuet, Palaiseau, France.
[c]Also at Università di Milano Bicocca, Milano, Italy.
[d]Also at Università di Bologna, Bologna, Italy.
[e]Also at Università di Modena e Reggio Emilia, Modena, Italy.
[f]Also at Novosibirsk State University, Novosibirsk, Russia.
[g]Also at Università di Ferrara, Ferrara, Italy.
[h]Also at LIFAELS, La Salle, Universitat Ramon Llull, Barcelona, Spain.
[i]Also at Università di Pisa, Pisa, Italy.
[j]Also at H.H. Wills Physics Laboratory, University of Bristol, Bristol, United Kingdom.
[k]Also at Università di Bari, Bari, Italy.
[l]Also at Sezione INFN di Trieste, Trieste, Italy.
[m]Also at Università di Genova, Genova, Italy.
[n]Also at Università degli Studi di Milano, Milano, Italy.
[o]Also at Universidade Federal do Triângulo Mineiro (UFTM), Uberaba-MG, Brazil.
[p]Also at AGH—University of Science and Technology, Faculty of Computer Science, Electronics and Telecommunications, Kraków, Poland.
[q]Also at Lanzhou University, Lanzhou, China.
[r]Also at Università di Padova, Padova, Italy.
[s]Also at Università di Cagliari, Cagliari, Italy.
[t]Also at MSU—Iligan Institute of Technology (MSU-IIT), Iligan, Philippines.
[u]Also at Scuola Normale Superiore, Pisa, Italy.
[v]Also at Hanoi University of Science, Hanoi, Vietnam.
[w]Also at P.N. Lebedev Physical Institute, Russian Academy of Science (LPI RAS), Moscow, Russia.
[x]Also at Università di Roma Tor Vergata, Roma, Italy.
[y]Also at Università di Roma La Sapienza, Roma, Italy.
[z]Also at Università della Basilicata, Potenza, Italy.
[aa]Also at Università di Urbino, Urbino, Italy.
[bb]Also at Physics and Micro Electronic College, Hunan University, Changsha City, China.
[cc]Also at School of Physics and Information Technology, Shaanxi Normal University (SNNU), Xi'an, China.